

18th International Conference on
Non-Conventional Materials and Technologies
"Construction Materials & Technologies for
Sustainability"
(18th NOCMAT 2019)
24th – 26th July 2019
Nairobi Kenya

FULL-CULM BAMBOO AS A FULL-FLEDGED ENGINEERING MATERIAL

Kent A. Harries^{1*}, Ian Nettleship¹, Yusuf Akinbade¹, Christopher Papadopoulos², Felipe Acosta², Johanna Morales Albino², and Mairim Ariezaga Gonzalez²

¹University of Pittsburgh, USA; kharries@pitt.edu ²University of Puerto Rico-Mayaguez, USA

*corresponding author

ABSTRACT

This paper provides an overview of the activities of a US National Science Foundation (NSF) funded project *Full-Culm Bamboo as a Full-Fledged Engineering Material* (Project Numbers NSF CMMI 1634739 and 1634828). The project, funded in 2017, is a collaboration between teams at the Universities of Pittsburgh and Puerto Rico Mayaguez.

KEYWORDS: bamboo, geometric properties, material properties, modelling, uncertainty

INTRODUCTION

The primary objective of this project is to establish the framework and tools required to standardize the evaluation of the material and mechanical properties of full-culm bamboo and thereby place bamboo on a similar footing to timber as a conventional building material. This research consolidates and significantly extends the extant body of knowledge and establish materials- and mechanics-based constitutive models for the behaviour of full-culm bamboo as a functionally graded, fibre-reinforced material. Three representations of bamboo behaviour are being developed forming the framework and tools required to evaluate the material and mechanical properties of bamboo for engineered applications. First, detailed analytical modelling is key to understanding the engineering properties of bamboo as a functionally graded material. An analytical model is being developed informed by innovative experimental methods focused on establishing through-wall and along-culm variation of fundamental mechanical properties. Second, surrogate representation of difficult-to-obtain engineering properties suitable for field test methods is necessary if broad adoption of full-culm bamboo is to be reliable. The approach taken leverages the analytical platform in order to develop both empirical and mechanics-based representations of engineering design properties that may be obtained from practical field tests. Finally, a new framework for modelling uncertainty in

bamboo material and mechanical properties, which can be highly variable, will enable reliable calibration of design equations. The approach includes stochastic generation of probability spatial distributions of mechanical properties implemented into the developed analytical model. The project advances the science of modelling both fibre reinforced and functionally graded materials. Indeed, a better understanding of the naturally evolved optimal design of the bamboo material and culm, including its nonhomogeneity and variability, will inspire optimization of other structural engineering functionally graded materials.

This paper reports work-in-progress and is intended to provide an overview of this NSF-funded project – the first of its kind funded by NSF – and to inspire others to develop similar data modelling techniques.

TRANSVERSE PHYSICAL AND MECHANICAL PROPERTIES OF BAMBOO

The circular cross section of bamboo is composed of unidirectional cellulosic fibres oriented parallel to the culm's longitudinal axis embedded in a parenchyma tissue matrix [1]. The parenchyma tissue matrix lignifies (hardens) as the culm matures leading to increased density and improved mechanical properties. As a functionally graded material, bamboo has evolved to resist its primary loading in nature: its own self-weight and the lateral effects of wind. The density of longitudinally oriented fibres increases from the inner culm wall to the outer culm wall [1]. The wall thickness is largest at the base of the culm and decrease with height up the culm. However, the size and quantity of vessels decrease with the height of the culm and are replaced with fibres. This addition of fibres compensates for loss in strength and stiffness due to reductions in diameter and wall thickness near the top of the culm, resulting in relatively uniform engineering properties along the entire culm height [2, 3].

Like any fibre-reinforced material, mechanical properties are highly correlated to the proportion and distribution of fibres in the cross section. Mechanical properties are influenced by density, which depends on fibre content, fibre diameter, and cell wall thickness [4]. The volume fraction of fibres ranges from approximately 60% at the exterior face of the culm wall to 10-15% near the interior face. The variation in density through the culm wall has been assumed by various researchers to be linear, quadratic, exponential, or a power function [5] and is known to be species-dependent [2, 6]. Due to the complex variation of the fibres and vascular bundles, the variation of material properties through the culm-wall thickness has been shown to be significant [7] and to have the effect of increasing gross culm stiffness by about 10% as compared to an assumed uniform distribution of the same volume of fibres [4]. A more refined analysis showed the effect of fibre gradient on gross culm stiffness to result in about a 5% increase for thin-walled culms (D/t < 8; P. edulis and Guadua angustifolia Kunth culms) and as much as 20% for thick-walled culms (D/t > 8; B. stenostachya culms) [3]. D is the culm outer diameter and t is the culm wall thickness.

In general, while highly variable, the longitudinal behaviour of bamboo is relatively well understood in a qualitative sense. From an engineering perspective, the longitudinal behaviour is most typically considered as a fibre-reinforced material in which longitudinal properties are obtained using a rule of mixtures approach. The dominant failure mode of bamboo however, is longitudinal splitting associated with bamboo carrying flexure, compression or tension loads. Janssen [8] describes the bending stresses in a culm as being characterised by the longitudinal compressive stress and transverse strain in the compression zone of the culm, with failure eventually occurring due to longitudinal splitting. This is ideally a Mode II longitudinal shear failure. However, in the presence of perpendicular stresses (as is the case where ever there is a

non-zero shear-to-moment ratio), there is some Mode I component stress which significantly reduces the Mode II capacity. Richard et al. [9] demonstrate the effects of such mode mixity, reporting Mode I capacities equal to only 18% of the Mode II capacity. Beam tests having mixed mode behaviour exhibited shear capacities ranging from 40-70% of the Mode II capacity.

Both the Mode I and II behaviours described are primarily functions of the transverse properties of the fibre-reinforced culm which are believed to be dominated by matrix (parenchyma) properties. However, despite their importance in the dominant observed behaviour of full-culm bamboo, there are few studies of the transverse properties of the culm wall. In early work, Arce-Villalobos [10] concluded that there is no correlation between the density of bamboo and its transverse tensile strength. Janssen [4], based on flexural tests, reports that a transverse strain of 0.0013 results in transverse tensile failure of the culm wall. More recently, test methods have been proposed for obtaining transverse properties of bamboo culms [11-13] although these have not yet been widely adopted to obtain material properties over a range of species and conditions.

The objective of the present study is to investigate the transverse material property gradient through the culm wall and to connect the mechanical behaviour to physical characteristics, such as fibre density. In this study, a modification to the flat-ring flexure [13] test specimen, in which only portions of the culm wall cross-section are tested, is used to obtain a measure of the transverse tensile capacity of the bamboo. Microscopy analyses are used to qualitatively describe the culm wall architecture and to quantitatively assess the failure modes through the culm wall thickness. Throughout this study, all position-dependent data are presented with respect to normalised culm wall thickness (x = 0 is the inner wall and x = 1 is the outer wall).

Five different bamboo species were tested in this study, *P. edulis*, *P. bambusoides*, *P. meyeri*, *P. nigra*, and *B. stenostachya*. All are thin-walled (D/t generally greater than 8) except *B. stenostachya* which is a thick-walled species. The moisture content of all specimens at time of testing was between 13% and 17%.

Fibre Distribution

Digital images of full culm wall cross sections were taken at each of the four quadrants (N, S, E and W). These images were processed using a purpose-built MatLab script to obtain the distribution of fibres through the wall cross section. An example of a collected image and resulting MatLab pixel map is shown in Figure 1. The image is divided in the through-thickness direction into ten equal regions of thickness t/10 (Figure 1b) and the fibre volume ratio obtained for each (Figure 1c). From this analysis, the average fibre distribution (expressed as third-order polynomial best-fit curves, each having a coefficient of determination $R^2 = 0.99$) is obtained as shown in Figure 1d and reported in Table 1. It is seen in Figure 1d that the fibre distribution among the four thin-wall *Phyllostachys* species is very similar. Indeed, a single relationship could be given for all four species having $R^2 = 0.96$. A marked difference in fibre distribution is observed in the thick-walled *B. stenostachya*. Thus, fibre distribution differs by genera but perhaps less so among species in the same genera.

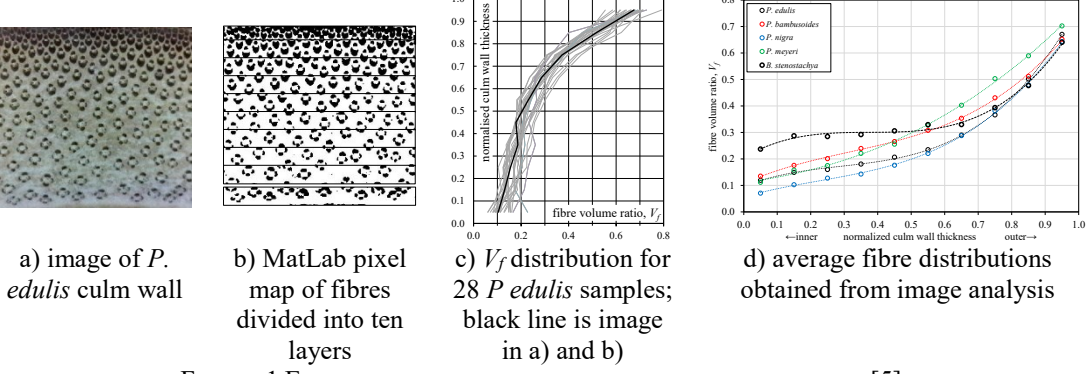


FIGURE 1 EXAMPLE OF DIGITAL IMAGE ANALYSIS OF CULM WALL [5].

Flat-ring Flexure Test

The flat ring flexure test [13] assesses the tendency of bamboo to fail via longitudinal cracks using a full cross-sectional specimen that is $L \approx 0.2D$ in length subjected to 4-point flexure as shown in Figure 2a. Due to the specimen geometry, the test gives the apparent modulus of rupture of the specimen (f_r), as if the specimen acts as a beam in flexure with its extreme points along the diameter parallel to the loading pins (labelled N and S in Figure 2b); this value therefore, corresponds to the transverse tension capacity of the bamboo. Prior to this study, the flat-ring flexure test has been used on only full culm cross sections. Such full-culm cross section specimens are referred to in this work as the control specimens and the modulus of rupture thus obtained is denoted f_{rC} .

Modulus of rupture, f_{rC} , determined for the full-culm control specimens is reported in Table 1. Within the genus *Phyllostachys*, these values are similar and notably greater than that observed for *B. stenostachya*. Observed variation of test results is typical of bamboo and similar to that reported previously [13].

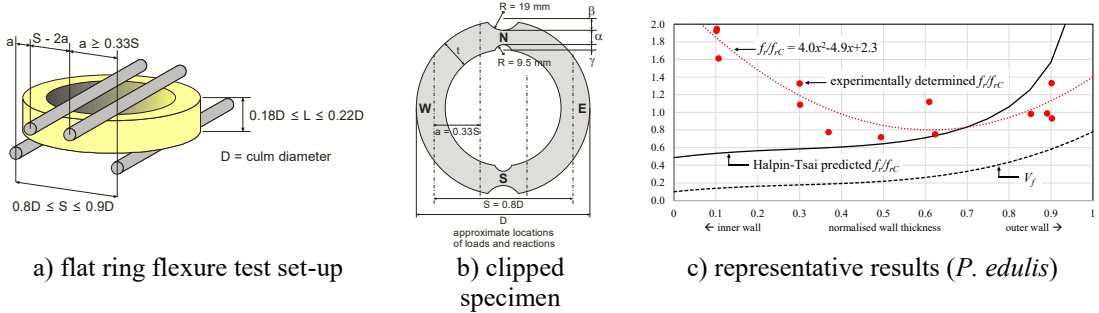


FIGURE 2 FLAT RING FLEXURE TEST, SPECIMEN AND REPRESENTATIVE RESULTS [5].

Clipped Flat-ring Test Specimens

This study adopts a modification to the flat-ring test specimen, in which only portions of the cross-section are tested in order to determine the effect of the material property gradient through the culm wall. 'Clipped' specimens (Figure 2b) had test regions machined using an end mill. Specimens were machined such that $\alpha \approx 0.20t$ or 0.25t and β and γ are in increments of approximately 0.20t or 0.25t such that the sum $\alpha + \beta + \gamma = t$, the culm wall thickness. This approach divides the culm wall into segments for which the modulus of rupture is determined from each segment and is assumed to represent the average value for that segment; the value is then assigned to the centroid of the segment.

An example of the experimentally determined values of normalised f_r/f_{rC} determined from the

clipped tests for *P. edulis* are shown in Figure 2c and the corresponding best fit second-order polynomial relationships for all species are reported in Table 1. These all illustrate a similar trend although *P. nigra* specimens exhibit relatively little variation through the culm wall compared to the other species.

| TABLE I SUMMART OF COLIN WALL FIBER DISTRIBUTION AND FLAT RING FLEXURE TEST RESULTS. | | | | | | | | | | | | |
|--|------------------------------------|---------------------|-----------------------|------------------------------|---------|---------------------|---|--|--|--|--|--|
| species | V_f | f _{rC} Mpa | fr/frC | $\int \frac{f_r}{f_{rc}} dx$ | frE/frC | δ_E/δ_C | $\frac{f_{rE}/\delta_E}{f_{rC}/\delta_C}$ | | | | | |
| P. edulis | $1.41x^3 - 1.23x^2 + 0.50x + 0.10$ | 17.3 | $4.0x^2 - 4.9x + 2.3$ | 1.18 | - | - | | | | | | |
| P. bambusoides | $0.96x^3 - 0.91x^2 + 0.57x + 0.10$ | 15.7 | $2.6x^2 - 2.5x + 1.5$ | 1.12 | 1.09 | 1.22 | 0.85 | | | | | |
| P. nigra | $0.94x^3 - 0.63x^2 + 0.36x + 0.06$ | 15.6 | $0.7x^2 - 0.8x + 1.4$ | 1.23 | 0.98 | 0.98 | 1.00 | | | | | |
| P. meyeri | $0.15x^3 + 0.34x^2 + 0.17x + 0.11$ | 20 | $2.4x^2 - 1.8x + 1.1$ | 1.00 | 0.93 | 1.27 | 0.70 | | | | | |
| R stanostachya | $1.75x^3$ $1.98x^2 + 0.75x + 0.20$ | 9.4 | $11v^2$ $36v + 16$ | 1 17 | 1.01 | 1.20 | 0.82 | | | | | |

TABLE 1 SUMMARY OF CULM WALL FIBER DISTRIBUTION AND FLAT RING FLEXURE TEST RESULTS.

Effect of Outer Layer of Bamboo Culm

Integrating the f_r/f_{rC} best-fit curves (Table 1) from x = 0 to x = 1 averages the local relative moduli across the section, and might be expected to represent the gross modulus across the section, i.e., the integral should equal unity. However, as shown in Table 1, with the exception of *P. meyeri*, the gross modulus obtained by integrating the clipped data exceeds unity by as much as 20%. A possible explanation for this behaviour – one in which the sum of the parts exceeds the capacity of the whole – is that failure of the full wall section control specimens is being initiated by a 'weak link'. A brittle failure of the outer layer of the culm wall initiating failure would explain this observation.

The extreme outer layer of a bamboo culm consists of a silica-rich outer skin (epidermis) and a thin region of densely packed fibres (this can be seen at the top of Figure 1a). It is believed that this layer will be more brittle than the rest of the culm wall and may help to initiate failures in specimens in which the outer wall is included. Therefore in the clipped specimen testing a question arises: is the outer layer contributing disproportionately to the observed behaviour, especially to the control and $\beta = 0$ tests? To investigate this effect, additional specimens were tested having $\beta \approx 0.05t$ and $\alpha \approx 0.95t$; essentially, these are full-culm sections with only the outer layer 'shaved' away. Flat ring flexure tests of this specimens having no epidermal layer were tested and the modulus of rupture, f_{rE} , and displacement of the loading points, δ_E determined. The ratios of these values to those obtained for full-culm control specimens are shown in Table 1. It is seen that the modulus of rupture, f_r , is essentially unaffected by the removal of the outer layer.

With the exception of *P. nigra*, the stiffness of the specimen is observed to decrease on the order of 15 to 30% upon the removal of the outer layer (Table 1). This decrease is greater than can be attributed to the loss of 5% of the moment of inertia of the cross section (resulting from shaving the specimen) alone.

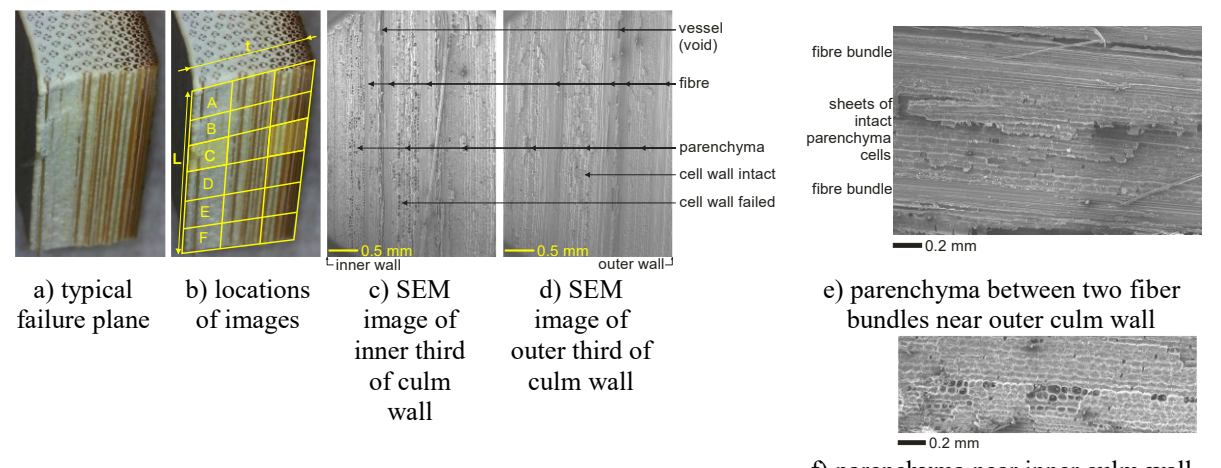
Discussion of Observed Transverse Behaviour

The data shown in Table 1 clearly indicate a parabolic distribution of modulus of rupture through the culm wall thickness with higher values at both the inner and outer walls and a minimum near the middle of the wall thickness. The fibre volume distributions, also shown in Table 1, indicate a typically observed distribution having few fibres at the inner wall and a greater number at the outer wall. Based on these fibre distributions, the predicted distribution of modulus of rupture using the Halpin-Tsai correction to the rule of mixtures [14] does not

appear to capture the experimentally observed behaviour, particularly in the inner half of the culm wall where fibre volumes are lowest (Figure 2c). Therefore, bamboo does not appear to behave as a classic fibre-reinforced composite material in the direction transverse to the fibres.

The observed behaviour requires further study and may represent a material variation or morphological variation through the bamboo culm wall thickness. To investigate this further, the fracture surfaces of full-culm wall thickness in control specimens (Figure 3a) were investigated using a scanning electron microscope (SEM). Each failure plane was divided into a grid (Figure 3b) and images of each obtained, allowing the entire failure plane to be imaged. The images shown in Figures 3c and 3d are typical of images obtained near the inner and outer walls, respectively, of a *P.edulis* specimen. These were obtained along grid section C (Figure 3b), slightly above the neutral axis of the section in flexure, in this case. Image features did not vary considerably based on their vertical location in the specimen (A to F in Figure 3b).

In Figures 3c and 3d the failure plane can be seen to both follow the edge of the fibre bundles and also to go through the bundles themselves. The fracture surface can be seen to expose the vessels (voids) surrounded by the bundle (near top of images in Figures 3c and 3d). Where it is seen, the interface between the parenchyma and the fibre bundle appears intact in most cases, indicating that the interface between fibres in the bundle is weaker than the interface between the fibres and parenchyma. Additionally, the parenchyma shown in Figures 3c and 3d, appear to be behaving differently. Near the outer culm wall (3d), the failure appears to follow the interfaces between parenchyma cells; however near the inner culm wall (3c), the failure plane often appears to pass through the parenchyma cells (seen as non-intact cell walls in the image). This observation is typical of all images obtained in this study. Indeed, near the outer culm wall, the parenchyma is typically observed to fail in 'sheets' of intact cells as shown in Figure 3e. In other images (Figure 3f) the intact parenchyma close to the inner culm wall appear 'desiccated': the intact cell wall appears to be 'caving in' or concave rather than being slightly 'inflated' or convex nearer the outer culm wall (Figure 3e). This observation may suggest a gradient in moisture content through the culm wall or a residual effect of moisture gradient during the drying process. Such a gradient should be expected. The bamboo culm epidermis is relatively impermeable and resistant to wetting whereas the inner culm wall is permeable [1, 15].



f) parenchyma near inner culm wall

FIGURE 3 DETAIL OF CULM WALL IMAGES OF P. EDULIS SPECIMEN

Figure 4 shows an SEM image of a typical P. edulis vascular bundle (near the outer culm wall) showing the fibre bundles surrounding the vessel and the parenchyma into which the bundle is embedded. In Figure 4, the fibre bundle can be seen to be penetrated by inter-fibre cracks whereas the interfaces between fibres and parenchyma appear quite intact. It is noted that the parenchyma cell walls are relatively thick indicating a relatively old culm age [16]. The cracking of the fibres may therefore be a function of culm age (observed although not described by [16]) or have formed as a result of shrinkage associated with drying the bamboo. A recent study [17] identified significantly varying morphology of parenchyma cell walls through the culm wall thickness of *P. edulis* samples. Near the outer culm wall, parenchyma cell walls were tightly packed laminar structures with little annular space at interstices. Nearer the inner culm wall, the laminar structure of the cell wall was separating and a larger annular space is present at parenchyma cell interstices. It is unclear how these differences impact behaviour illustrated in Figure 3 but it is evident that parenchyma is not homogeneous through the cross section. Neither [16] nor [1] provide insight on the source of this inhomogeneity and the present authors can only speculate on its cause, although it does appear to affect the through thickness mechanical behaviour of the culm wall.

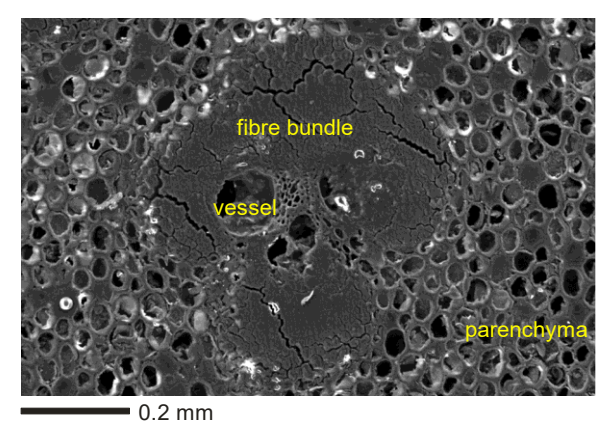


FIGURE 4 SEM IMAGE OF P.EDULIS VASCULAR BUNDLE

QUANTIFICATION OF MATERIAL VARIABILITY

As described above, the variation of bamboo through-culm wall properties is of interest. Such data will be used to quantify uncertainty in finite element modelling full-culm bamboo. The variation of constituent bamboo strips in glue-laminated bamboo application is also of interest to manufacturers of these products. Image analysis was used to quantify the distribution of fibre volume ratio, V_f , in strips of P. edulis bamboo used in commercially available glue-laminated bamboo structural elements.

High resolution images of cross sections of 60 glue-laminated bamboo beams were obtained. The images used in this study are those produced by Penellum et al. [17], an example is shown in Figure 5a. The commercially obtained beams – obtained from two different manufacturers (denoted M and P) – had been previously tested in flexure. The beams were fabricated from bamboo strips each of which was 19 mm wide and 6 mm thick in the direction through the culm wall. Over 3600 individual images of the 19 mm x 6 mm strips were extracted from the 60 beam section images available. Each image is approximately 900 x 300 pixels corresponding to a pixel resolution of approximately 2400 pixels/mm², equivalent to 1200 dpi (this is available on a standard document scanner). Approximately 13% of the extracted images were excluded from further analysis due primarily to poor image quality. Additionally, approximately 3% of the strip sections were near the bamboo nodal region; the varying fibre orientation and bamboo

morphology in this region is also unsuitable for the analysis conducted and so these strips were also excluded from further analysis.

Using a purpose-written MatLab script, each image was divided into ten equal sub images in the through-culm wall 6 mm direction (similar to the manner shown in 1). The fibre components were extracted from the images based on contrast and the fibre volume ratio determined. From this analysis the total fibre volume ratio of each strip, V_f , and the distribution as a function of location in the strip can be determined. Figures 5b and 5c shows examples of data obtained for M and P strips, respectively.

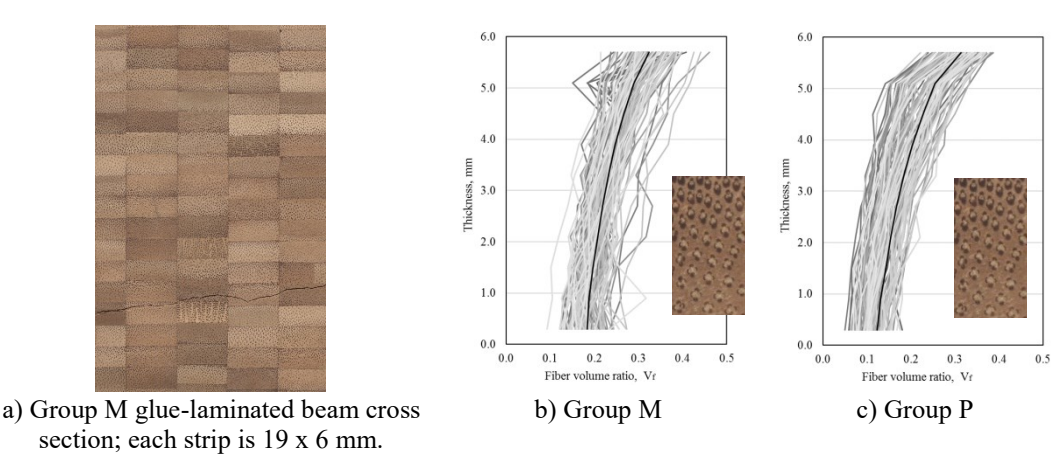


FIGURE 5 REPRESENTATIVE FIBER VOLUME DISTRIBUTIONS FROM 100 STRIPS.

Total fibre volume ratio, V_f obtained is given in Table 2. Distribution of fibre volume ratio through the culm wall thickness is not meaningful in so far as the actual location of the 6 mm sample within the culm wall is unknown. Nonetheless, the nature of the distribution and its variation is a measure of the uncertainty inherent in ascribing geometric or material properties to bamboo. Each acquired fibre distribution was fitted to both a linear $(V_f = mx + b)$ and exponential relationship $(V_f = be^{mx})$. The value of m, in each case, describes the variation of the fibre volume across the strip dimension x which ranges from 0 to 6 mm. The value b is not addressed as this is a function of the location of the 6 mm strip within the culm wall and is not uniquely defined in this study. The values of m determined are given in Table 2.

TABLE 2 SUMMARY OF FIBER VOLUME RATIO AND DISTRIBUTIONS DETERMINED FROM IMAGE ANALYSIS.

| Group | n | fibre volume ratio | | $V_f = mx + b$ | | $V_f = be^{mx}$ | | |
|-------|------|--------------------|-------|----------------|------|-----------------|-------|--|
| | | mean V_f | COV | mean m | COV | mean m | COV | |
| M | 2450 | 0.235 | 0.130 | 0.025 | 0.32 | 0.105 | 0.315 | |
| P | 603 | 0.190 | 0.191 | 0.032 | 0.25 | 0.172 | 0.296 | |
| M+P | 3053 | 0.226 | 0.160 | 0.026 | 0.31 | 0.118 | 0.387 | |

Further work is necessary to automate the calculation of fiber volume ratio distribution in bamboo sections, particularly to conduct it directly on intact specimens. As of the writing of this article, another purpose-written MatLab script has been developed, but not yet verified, that can measure fiber volume ratio in each segment of an arbitrary "polar grid" that divides a full culm section circumferentially and through the thickness.

NUMERICAL MODELING

At the time of writing, limited progress had been made in modelling the bamboo culm wall. Linear finite element models (FEM) of the flat ring flexure specimen are developed using ABAQUS based on the results presented above. These have been validated using both flat ring flexure and circumferential compression tests [12] which use the same specimen geometry. Digital image correlation (DIC) is used in some tests (Figure 6a) to obtain full field strain data during testing. FEM complexity is also being considered with results for three modelling scenarios being considered.

Case 1: a model to which gross section material properties are assigned. While simple, such an approach does not capture the graded nature of the culm wall. An effect of this is seen in Figure 6c in which the strain gradient passes through zero at the section elastic neutral axis rather than being shifted toward the outer culm wall.

Case 2: divides the culm wall into ten concentric sections and assigns these material properties based on the approach described above in Figure 2 and Table 1.

Case 3: assigns material properties through the culm wall using similar distributions as Case 2 but using a continuum approach (graded elements) assigning properties to integration points through the culm wall thickness. This approach mitigates some of the error anticipated using discrete steps in Case 2 and will lead to smooth strain fields [19]. This approach is implemented using the ABAQUS USDFLD subroutine. Once validated, this routine will be made freely available to the bamboo research community.

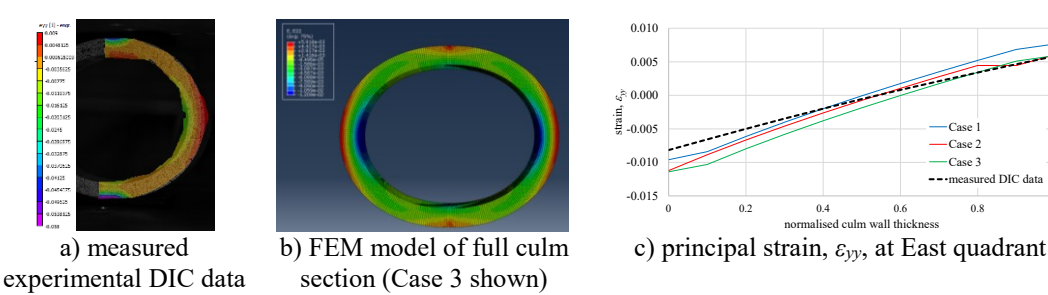


Figure 6 Numeric modeling of bamboo circumferential compression tests showing results for vertically oriented strain, ε_{vv} .

As the modelling tasks progress, the effects of uncertainty in bamboo microstructure will be integrated into the model. One objective of this activity is to begin to quantitatively understand the variation in tested bamboo materials properties – particularly why some test methods exhibit less variation than others [7, 9].

CONCLUSIONS

Performance of full-culm bamboo structures is dominated by longitudinal splitting behaviour which is a function of the transverse properties of this highly orthotropic material. Considerable study of the longitudinal properties of bamboo is available; a primary hypothesis of much of this work is that bamboo may be considered as a fibre-reinforced composite material and material properties may be assessed using rule-of-mixture methods. Nonetheless, few studies have addressed the transverse properties of the bamboo culm wall, despite these largely governing full-culm behaviour. This study investigates the transverse material property gradient through the culm wall and attempts to connect the mechanical behaviour with physical characteristics. Most importantly, the study demonstrates that the transverse behaviour is complex and that bamboo does not appear to behave as a classic fibre-reinforced composite material in the direction transverse to the fibres.

A primary objective of this project is to develop a framework and tools required to standardize the evaluation of the material and mechanical properties of full-culm bamboo. The variation inherent in bamboo from species to species and location to location is significant. The validated modelling tools developed will be shared and refined for use in a variety of international contexts so that they can be used to better interpret the considerable range of materials test data available. Coupled with a materials informatics approach [19], the opportunities for bamboo materials refinement and discovery are significant and – it is hoped – will help draw bamboo to the same degree of acceptance as comparable 'conventional' building materials.

ACKNOWLEDGEMENTS

This research was partially funded through National Science Foundation Awards 1634739 and 1634828 *Collaborative Research: Full-culm Bamboo as a Full-fledged Engineering Material*.

REFERENCES

- [1] Liese, W. (1998) The Anatomy of Bamboo Culms, Brill. 204 pp.
- [2] Amada, S., Munekata, T., Nagase, Y., Ichikawa, Y., Kirigai, A. and Zhifei, Y. (1996) The mechanical structures of bamboos in viewpoint of functionally gradient and composite materials, *Journal of Composite Materials*, **30**, 800-819.
- [3] Harries, K.A., Bumstead, J., Richard, M.J. and Trujillo, D. (2017) Geometric and Material Effects on Bamboo Buckling Behaviour, *ICE Structures and Buildings* Themed issue on bamboo in structures and buildings, **170**(4), 236-249.
- [4] Janssen, J.J.A., (2000) *Designing and Building with Bamboo*, INBAR Technical Report 20. International Network for Bamboo and Rattan, Beijing, China.
- [5] Akinbade, Y., Harries, K.A., Flower, C., Nettleship, I., Papadopoulos, C., and Platt, S.P. (in review) Determining Through-Culm Wall Distribution of Mechanical Properties of Bamboo, *Construction and Building Materials*
- [6] Amada, S., Ichikawa, T., Munekata, T., Nagase, Y., and Shimizu, H., (1997) Fiber texture and mechanical graded structure of bamboo, *Composites: Part B*, **28B**, 13-20.
- [7] Richard, M.J., Harries, K.A., (2015) On Inherent Bending in Tension Tests of Bamboo, *Wood Science and Technology* **49**(1) 99-119.
- [8] Janssen, J. (1981) *Bamboo in Building Structures*. Doctoral Dissertation, Eindhoven University of Technology, Netherlands.
- [9] Richard, M., Gottron, J., Harries, K.A. and Ghavami. K. (2017) Experimental Evaluation of Longitudinal Splitting of Bamboo Flexural Components, *ICE Structures and Buildings* Themed issue on bamboo in structures and buildings, **170**(4), 265-274
- [10] Arce-Villalobos O.A. (1993) Fundamentals of the design of bamboo structures, Master's thesis, Eindhoven University of Technology, The Netherlands.
- [11] Mitch, D., Harries, K.A., and Sharma, B. (2010) Characterization of Splitting Behavior of Bamboo Culms. *ASCE Journal of Materials in Civil Engineering*, **22**, 1195-1199.
- [12] Sharma, B., Harries, K.A. and Ghavami, K. (2012) Methods of Determining Transverse Mechanical Properties of Full-Culm Bamboo, *Journal of Construction and Building Materials*, **38**, 627-637.
- [13] Virgo, J., Moran, R., Harries, K.A., Garcia, J.J., and Platt, S. (2017) Flat Ring Flexure Test for Full-Culm Bamboo, *Proceedings of 17th International Conference on Non-Conventional Materials and Technologies (17NOCMAT)*, Yucatán, México, November 2017.
- [14] Halpin, J.C. and Kardos, J.L. (1976) The Halpin-Tsai Equations: A Review, *Polymer Engineering and Science* **16**(5), 344-352.
- [15] Yao, L.H., Wang, X.M. and Fei, B.H. (2011) Study on Permeability Coefficient of Different Bamboo/Fir Veneer Surface, *Advanced Materials Research*, **311-313**, 1634-1637.
- [16] Liese, W. and Weiner, W. (1996) Ageing of Bamboo Culms. A Review. *Wood Science and Technology*, **30**, 77-89.

- [17] Zheng, Q., Zhang, Q., Lu, Q., Zhou, Y., Chen, N., Rao, J. and Fan, M. (2019; in press) Wetting behavior and laminate bonding performance of profiled tangential surfaces of moso bamboo, *Industrial Crops and Products*
- [18] Penellum A, Sharma B, Shah D.U, Foster R.M, Ramage M.H. (2018) Relationship of structure and stiffness in laminated bamboo composites. *Construction and Building Materials* **165**, 241-246
- [19] Silva, E,C,N, Walters, M.C. and Paulino, G.H. (2006) Modeling bamboo as a functionally graded material: lessons for the analysis of affordable materials, Journal of Materials Science, 41(21), 6991–7004.
- [20] Zheng, C., Akinbade, Y., Nettleship, I. and Harries, K.A. (2019) The Potential Utility of Materials Informatics in Developing Non-Conventional Materials, *18th International Conference on Non-Conventional Materials and Technologies (18NOCMAT)* Nairobi, Kenya, July 2019.